Adjusting Mitigation Pathways to stabilize climate at 1.5 and 2.0 °C rise in global temperatures to year 2300

P. Goodwin[1], S. Brown[2], I.D. Haigh[1], R.J. Nicholls[2], and J.M. Matter[1]

[1]Ocean and Earth Science, University of Southampton, National Oceanography Centre Southampton, Southampton, SO14 3ZH. United Kingdom.

[2]Faculty of Engineering and the Environment and Tyndall Centre for Climate Change Research, University of Southampton, Highfield, Southampton. SO17 1BJ. United Kingdom.

Author ORCID IDs:

Goodwin: ID 0000-0002-2575-8948
Brown: ID 0000-0003-1185-1962
Haigh: ID 0000-0002-9722-3061
Nicholls: ID 0000-0002-9715-1109
Matter: ID 0000-0002-1070-7371

Manuscript re-submitted to *Earth's Future*
23rd January 2018

Accepted for publication in *Earth's Future*
27th February 2018

This is the Author Accepted Manuscript

Key Points

- Adjusting Mitigation Pathway scenarios are defined for climate stabilization at 1.5, 2, 2.5, 3 and 4.5 °C above preindustrial to year 2300.
- Our study provides a flexible framework for policy makers to reach agreed climate stabilization targets following the INDC Paris Agreement period.
- Median projection suggest that annual carbon emissions must be reduced to zero by 2045 for 1.5 °C, and by the 2080s for 2.0 °C.
- Reduction in future sea level rise is up to 4m by year 2300 for a 1.5°C target compared to a high-end scenario.

Abstract

To avoid the most dangerous consequences of anthropogenic climate change, the Paris Agreement provides a clear and agreed climate mitigation target of stabilizing global surface warming to under 2.0 °C above preindustrial, and preferably closer to 1.5 °C. However, policy makers do not currently know exactly what carbon emissions pathways to follow to stabilize warming below these agreed targets, because there is large uncertainty in future temperature rise for any given pathway. This large uncertainty makes it difficult for a cautious policy maker to avoid either: (1) allowing warming to exceed the agreed target; or (2) cutting global emissions more than is required to satisfy the agreed target, and their associated societal costs. This study presents a novel Adjusting Mitigation Pathway (AMP) approach to restrict future warming to policy-driven targets, in which future emissions reductions are not fully determined now but respond to future surface warming each decade in a self-adjusting manner. A large ensemble of Earth system model simulations, constrained by geological and historical observations of past climate change, demonstrates our self-adjusting mitigation approach for a range of climate stabilization targets ranging from 1.5 to 4.5 °C, and generates AMP scenarios up to year 2300 for surface warming, carbon emissions, atmospheric CO_2, global mean sea level, and surface ocean acidification. We find that lower 21st century warming targets will significantly reduce ocean acidification this century, and will avoid up to 4m of sea-level rise by year 2300 relative to a high-end scenario.

1. Introduction

There is uncertainty in the response of the climate system to any given future scenario, shown by the wide warming responses of climate models (IPCC, 2013) when forced with the same prescribed forcing pathways (Meinshausen et al., 2011a). This uncertainty in warming response makes it difficult to prescribe a future pathway now, that will limit future warming to satisfy the Paris Climate Agreement (UNFCCC, 2015) target over the 21st century of under 2.0 °C above preindustrial (e.g. IPCC, 2013; Meinshausen et al., 2009), and preferably closer to 1.5 °C. For example, some of the Climate Model Intercomparison Project phase 5 (CMIP5) ensemble of complex Earth system models suggest that the prescribed Representative Concentration Pathway 4.5 (RCP4.5) will lead to warming of less than 2 °C, while other ensemble members suggest that 2 °C will be exceeded even if the more heavily mitigated RCP2.6 pathway is adopted (IPCC, 2013). Thus, at this point in time we do not know exactly which pathway to follow to stabilize global mean surface warming to a given target, such as the 1.5 or 2.0 °C targets of the Paris Climate Agreement (UNFCCC, 2015).

The highly complex CMIP5 models are too computationally expensive to conduct full parameter space exploration of the uncertainty in pathways that lead to stabilization at 1.5 or 2.0 °C warming, and to run simulations beyond 2100. To investigate questions where computational expense prohibits using highly-complex models, one approach has been to generate an ensemble using an efficient model, where the input parameters are tuned to emulate a more complex model ensemble, for example using the MAGICC6 efficient climate model to emulate the CMIP3 ensemble (Meinshausen et al., 2011b; 2011c). Here we take an alternative approach, used by Goodwin et al. (2018), based on history matching (Williamson et al., 2013; 2015): we generate a large Monte Carlo ensemble of many millions of efficient climate model simulations with varied input parameters, using geological evidence for the input distribution of the climate sensitivity (Rohling et al, 2012), and then select only those simulations that agree with historical observations to make future projections. This results in a large ensemble of observation-consistent climate simulations with computational efficiency to project hundreds of years into the future.

Goodwin et al. (2018) applied this method to evaluate the amount of carbon that can be emitted before the 1.5 and 2.0 °C warming targets are breached, using four RCP scenarios to integrate into the future. Goodwin et al. (2018) used observational reconstructions of surface

96 warming, ocean heat uptake and atmosphere-ocean-terrestrial carbon fluxes up to the end of year 2016 to extract observation-consistent simulations via the history matching (Williamson
98 et al, 2013; 2015). The final history matched model ensemble contains many thousands of simulations, and has warming projections similar to, but narrower than, the CMIP5 ensemble
100 (Goodwin et al, 2018, see figure 2 therein). This final history matched ensemble contains simulations that are not only consistent with historical observations of warming, heat uptake
102 and carbon fluxes; the simulations also span the observational uncertainty.

104 Goodwin et al. (2018) found that if the total carbon emitted after the start of 2017 reaches 135 PgC, there is a 95% chance that warming remains under 1.5 °C. This likelihood drops to 66%
106 if emissions reach 200PgC and to just 5% if emissions reach 325 PgC (Goodwin et al., 2018). For the higher Paris Agreement target, if the total carbon emitted after 2017 reaches 315 PgC
108 there is a 95% chance that warming will remain under 2.0 °C, reducing to 66% if emissions reach 405 PgC and 5% if emissions reach 590 PgC. These results for the cumulative carbon
110 emitted when warming targets were breached were similar following different RCP scenarios (Goodwin et al. 2018), in spite of the difference in non-CO2 radiative forcing, consistent with
112 a near-linear link between cumulative emissions and warming (Allen et al., 2009; Gillet et al., 2009; Goodwin et al, 2015).
114
Given these projected emission limits (Goodwin et al., 2018), and a current annual rate of
116 carbon emission of over 11 PgC per year (le Quéré et al., 2016), only scenarios where mitigation is immediate and comprehensive will likely restrict 21st century warming to a
118 maximum of 1.5 to 2.0 °C above preindustrial in Earth system models, such as the RCP2.6 scenario (IPCC, 2013). However, the uncertainty in the future climate response to emissions
120 makes it difficult to prescribe now a precise emissions policy that will avoid either possible societal costs from warming exceeding an agreed warming target, or possible societal costs
122 from emissions being cut further than required to meet the agreed warming target. Will the real climate system remain under 1.5 °C until total future emissions reach 135 PgC, or 200
124 PgC, or even 325 PgC?

126 As the 21st century progresses, the extended observational records will reduce uncertainty in the future warming for a given emissions pathway, and will provide extended records on
128 anthropogenic emissions. However, the emissions pathways available will also narrow over time, increasing the likelihood of it becoming impossible to limit warming to under 2 °C.
130 Thus, to maximize the chance of restricting warming to an agreed target, an immediate future pathway to reduce the emission rate must be adopted as soon as possible, based on current
132 understanding. Then, this emissions policy can be adjustted as the ongoing observational record reduces uncertainty over the 21st century.
134
This study explores an innovative self-adjusting approach to mitigation, in which an agreed
136 policy framework is adopted defining how quickly the global carbon emission rate is reduced based on decadal re-assessment of the future realized warming trajectory over the 21st
138 century. An efficient Earth system model is used to test this adjusting approach to mitigation for climate stabilization targets between 1.5 °C and 4.5 °C above preindustrial, and generate
140 scenarios for warming, atmospheric CO_2, surface ocean *p*H and global mean sea-level (GMSL) rise for the different climate stabilization targets. Importantly, we extend our future
142 scenarios to year 2300 since the climate stabilization target will have impacts, on for instance the extent of sea-level rise, well beyond the 21st century.
144
The adjusting mitigation approach used here has similarities to, but is distinct from,
146 adaptation pathways that have been applied in the impacts and adaptation literature (e.g. Haasnoot et al. 2013; Barnett et al. 2014; Ranger et al. 2013). Adaptation pathways for
148 impacts and adaptation address deep uncertainty in both the climate system and human impacts through a series of linked adaptive actions triggered by changes in external conditions
150 that lead to a low-regrets future through adaptive management (Haasnoot et al. 2013; Barnett

et al. 2014; Ranger et al. 2013). In an adaptation pathway, a tipping point occurs, and triggers an adaptive action to switch to an alternative pathway to reduce risk to the whole system, for example an increase in the rate of sea-level rise in the Thames Estuary above some threshold may alter the planning strategy for flood defences (Nicholls et al. 2013; Ranger et al. 2013). This addresses deep uncertainty by having an overall adaptation management goal, but allowing time to resolve highly uncertain events where a step-change in management in require to reach that goal. In contrast, in the self-adjusting mitigation pathways considered here the climate stabilization target is fixed at the outset with no further adaptive decisions to change this climate stabilization target. The goal is not to over-mitigate or under-mitigate to an uncertain sensitivity of warming to emissions. Therefore, our adjusting mitigation pathways approach considers only the uncertainty in the physical climate system, regarding the emissions required to reach a climate stabilization target, and does not consider uncertainty in the human impacts of the resulting climate change. Adaptive pathways can be framed in terms of 'signposts', which are measured quantities of the climate system, and tipping points or 'triggers', which are used to determine whether policy should be adapted (e.g. Haasnoot et al., 2013). Here, the self-adjusting mitigation pathway approach does also contain 'signposts', since the global mean temperature and emission rates are monitored. However, the approach here differs from an adaptation pathways in that are no 'triggers' at which a response is or is not taken. Rather, here the emissions pathway is continually adjusted based on the observations to maintain the same policy target for global mean surface warming. This does not avoid the evitable 'lock-in' as we are already committed to sea-level rise due to past emissions. However Adjustable Mitigation Pathways indicate potential further lock-in and suggest the pathways for implications of further emission reductions, which helps guide adaptation response.

Section 2 of this paper presents and tests an algorithm that continually re-assesses how quickly to reduce the global carbon emission rate based on how the realized warming trajectory unfolds over the 21st century and beyond, and then adjusts the mitigation pathway to continually aim for a climate stabilization target defined at the outset. The algorithm is employed to define five Adjusting Mitigation Pathway (AMP) scenarios, which are employed within a large ensemble of simulations using the Warming Acidification and Sea-level Projector (WASP) Earth system model (Goodwin, 2016). The WASP model configuration of Goodwin et al (2018) is used, containing monthly time-step and stochastic temperature variability, with the additional sea level component included after Goodwin et al. (2017). The AMP1.5 scenario represents eventual climate stabilization at 1.5 °C above preindustrial, where preindustrial is taken here to be approximated by the 1850-1900 time period and be 0.78 °C below the 1993-2012 global mean surface temperature (IPCC, 2013). The AMP2.0, AMP2.5, AMP3.0 and AMP4.5 scenarios represent policy aims for eventual climate stabilization at targets of 2.0 °C, 2.5 °C, 3.0 °C and 4.5 °C warming above preindustrial respectively.

Section 3 of this paper then presents the AMP scenarios in the WASP model ensemble for carbon emissions, surface warming, atmospheric CO_2, surface ocean acidification and GMSL rise, up to year 2300 for the different climate stabilization targets. The ability of these AMP scenarios to reach the required climate stabilization target are assessed, by considering the robustness of the AMP scenarios. Future projections from the AMP scenarios are compared to the high-end prescriptive RCP8.5 scenario, and it is found that adoption of a climate stabilization target policy now will significantly reduce ocean acidification during the 21st century, and significantly reduce GMSL rise by year 2300.

Section 4 discusses the implications of this study. The full AMP scenarios for emissions, warming, atmospheric CO_2, surface ocean acidification and sea-level rise defined and described here are given in Electronic Supplementary Information.

2. Methods

This section presents our novel Adjusting Mitigation Pathway (AMP) approach to restrict warming to a given climate stabilization target, testing the AMP approach in a large ensemble of Earth system model simulations.

2.1 Generating the ensemble climate simulations

The WASP Earth system model is used (Goodwin, 2016; Goodwin et al., 2017), comprising a computationally efficient 8-box representation of the atmosphere-ocean and terrestrial carbon system. WASP calculates the global surface temperature anomaly from cumulative carbon emissions based on the equation of Goodwin et al. (2015), with additional terms for radiative forcing from other sources (Goodwin, 2016; Williams et al., 2016; 2017). Here, we use the WASP configuration of Goodwin et al. (2018), containing a monthly time-step and with added stochastic surface temperature anomaly, forced by Auto Regressive, AR(2), noise where the coefficients are set to approximate the monthly temperature variability shown by the GISTEMP record (GISTEMP 2017; Hansen et al., 2010). We also include the hybrid method for projecting global mean sea-level rise as described in Goodwin et al. (2017), with thermosteric sea-level rise calculated from the simulated ocean heat uptake after Williams et al. (2012) and an ice-melt contribution calculated from a semi-empirical coefficient (Rahmstorf, 2007).

The added stochastic inter-annual temperature anomaly tests whether the AMP framework can adapt the emissions pathway to reach the required warming target even though the observed time-average warming reflects both the trend in warming and inter-annual variability (Figure 1).

Exploiting the computational efficiency of WASP, an initial ensemble of 5×10^7 simulations is generated using a Monte Carlo approach (Goodwin, 2016; Goodwin et al., 2017), with each simulation containing a unique set of model parameter values (Supplementary Table 1). The simulations are restored to historic CO_2 concentrations from year 1765 to 2005. From year 2005 to year 2014 each simulation is forced with the global annual carbon emission rate from the Global Carbon Budget (Boden et al., 2016; Houghton et al., 2012; Le Quéré, 2016). From 2015, the global annual carbon emission rate is then linearly interpolated towards the year 2030 from the Paris Agreement 'Intended Nationally Determined Contributions' (INDC) global carbon emissions (Fawcet et al., 2015).

The WASP Earth system model does not have interactive cycles of non-CO_2 radiative forcing agents, such as methane, nitrous oxides, halogens or aerosols. Therefore, in the simulations forcing agents other than CO_2 are prescribed following historic values and then into the future by the heavily mitigated scenario, RCP2.6 (Meinshausen et al., 2011). The uncertainty in the radiative forcing from these other agents is tuned to the present-day uncertainty and scaled over time (Supplementary Table 1). A total of 19 model parameters are varied between the 5×10^7 simulations (Supplementary Table 1), including the equilibrium climate sensitivity, the timescales of ocean tracer uptake, the terrestrial carbon cycle sensitivity to warming and CO_2 and the ice-melt sensitivity to warming.

A subset of the initial 5×10^7 simulations are chosen for the final model ensemble, and used to make future projections, following the methodology of Goodwin (2016) and Goodwin et al. (2017). To extract the simulations for the final ensemble, each of the initial 5×10^7 simulations is assessed for observational consistency against 10 metrics of observed climate change when the simulations reach the start of year 2017 (Supplementary Table 2). The 10 metrics include observed surface warming (GISTEMP, 2017; Hansen et al., 2010; IPCC, 2013; Morice et al., 2012; Smith et al., 2008; Vose et al, 2012), ocean heat uptake (Cheng et al, 2017; Levitus et al, 2012; Smith & Murphy, 2007; Smith et al., 2015), ocean and terrestrial carbon uptake (IPCC, 2013), and GMSL rise (IPCC, 2013). This leaves just 5,784 simulations that satisfy the historic consistency tests, and only these simulations are then used to integrate forward in time to year 2300 and define the AMP scenarios. It should be noted that WASP ensemble

members generated for this study are observationally constrained to only include only processes that have acted historically (e.g. Goodwin et al. 2017), and therefore historically unprecedented processes that may act in the future are not considered in the simulations. Historically unprecedented processes could affect future warming, required carbon emissions or sea-level rise trajectories in a way not included within our simulations, for example due to a possible historically unprecedented sudden change in ice sheet dynamics (Kopp et al., 2017).

This extraction of a historically plausible subset of simulations (Supplementary Tables 1 and 2), from a large initial Monte Carlo ensemble, produces a final ensemble of future projections from the efficient WASP model with future warming and GMSL sensitivities that are similar to more complex and computationally expensive Earth system models (Goodwin, 2016; Goodwin et al., 2017). Here, we utilize this computational efficiency to generate and test our AMP scenarios, including uncertainty ranges, for climate stabilization targets between 1.5 °C and 4.5 °C above preindustrial out to year 2300.

2.2 Adjusting Mitigation Pathway framework for climate stabilization

This section presents an algorithm for determining the required carbon emissions reductions to stabilize warming at an agreed policy target, based on decadal assessment of the observed future-warming trajectory.

The AMP scenarios first assume that global carbon emissions follow the 'Intended Nationally Determined Contributions' (INDC) from the Paris Agreement until year 2030 (Fawcet et al., 2015). To achieve this, the annual carbon emission rate is linearly increased from the year 2017 value to the Fawcet et al. (2015) figure for 2030 (Figure 1). From the year 2030, the AMP scenarios reduce the carbon emission rate linearly over time to restrict warming to the climate stabilization target, assuming that warming is approximately linearly related to the cumulative carbon emission (Allen et al, 2009; Gillet et al., 2013; Goodwin et al., 2015; Matthews et al., 2009). The AMP algorithm makes assessments of the required reduction in the carbon emission rate for climate stabilization n=9 times between 2030 and 2125: starting every ten years from time t_1=2030 to time t_8= 2100, and then a final assessment made at year t_9=2125 (Figure 1).

The algorithm assesses the required reduction in carbon emissions for climate stabilization as follows. First, the additional warming per unit additional carbon emitted, $((\Delta T/\Delta I)_{obs}$, in °C/1000PgC), is calculated at time t_n from realized trajectory global surface temperature anomaly, ΔT, and the change in cumulative carbon emissions, ΔI_{em} in PgC, by comparing a 10-year period (t-11 years to t-1 year) relative to the 2003-2012 average using,

$$\left.\frac{\Delta T}{\Delta I}\right|_{obs}\left(t_n\right)=\frac{\overline{T}\left(t=t_n-11\rightarrow t_n-1\right)-\overline{T}\left(t=2003\rightarrow 2012\right)}{I_{em}\left(t=t_n-5\right)-I_{em}\left(t=2008\right)} \quad . \qquad (1)$$

Note that in eqn. (1) the 10-year observation period (t=t_n-11 to t_n-1) ends 1 year prior to the time when the rate of emissions reductions is altered (t_n), to facilitate time for policy agreement and implementation.

Next, the remaining cumulative CO_2 emission allowed after time t_n, $I_{remaining}(t_n)$ in PgC, to restrict total warming to the policy-determined target, ΔT_{aim}, is calculated. This is achieved assuming that there is a near-linear link between additional cumulative carbon emitted and future warming (Allen et al., 2009; Gillet et al., 2013; Matthews et al., 2009; Goodwin et al., 2015). This near-linear link implies that the observed additional warming per unit emission, $(\Delta T/\Delta I)_{obs}$ (eqn. 1), continues into the future, giving

$$I_{remaining}(t_n) = \left[\Delta T_{aim} - \Delta\overline{T_{obs}}(t_n)\right] \Big/ \left[\left.\frac{\Delta T}{\Delta I}\right|_{obs}(t_n)\right], \quad (2)$$

where the observed temperature anomaly at time t, $T_{obs}(t)$, is calculated assuming that the 2003 to 2012 period was 0.78 °C above preindustrial (IPCC, 2013),

$$\Delta T_{obs}(t_n) = \Delta\overline{T}(t = t_n - 11 \rightarrow t_n - 1) - \Delta\overline{T}(t = 2008 \rightarrow 2012) + 0.78 .$$

The annual global net carbon emission rate is then linearly reduced to zero so that total future cumulative emission after time t_n is $I_{remaining}(t_n)$ using,

$$C_{rate}(t) = C_{rate}(t_n)\left(1 - \frac{t - t_n}{t_{C=0}}\right), \quad (3)$$

until t-t_n = $t_{C=0}$, where $t_{C=0}$ = $2I_{remaining}(t_n)/C_{rate}(t_n)$ is the time at which the carbon emission rate is reduced to zero.

It should be noted that in the Adjusting Mitigation Pathway algorithm (eqns. 1-3) the final value for $I_{remaining}(t_n)$ (eq. 2) will only be known 1-year before the rate of emission reductions is adjusted (eq. 3). In practice, however, policy makers will have more time to prepare for the adjustments than this, since half the data required to calculate the ten-year time average temperature anomaly (eq. 1), and $I_{remaining}$ (eq. 2), will be available 6 years prior to the point at which the rate of emission reductions is adjusted. From 6-years prior to the implementation of adjustments to emissions reductions, the estimated value of $I_{remaining}$ from partial data will be continually improved until the value is finalized at 1-year prior to t_n.

Once emissions have been reduced to zero, t-t_n>$t_{C=0}$ (eq. 3), a check on the simulated temperature anomaly, $T_{obs}(t)$, relative to the warming target. ΔT_{aim} is undertaken at each model time-step. To maintain warming close to the stabilization target, a small regulating emission rate is permitted: negative emissions of -1.0 PgC yr^{-1} are applied if $T_{obs}(t)$ is more than 0.05 °C above ΔT_{aim}, and positive emissions of +1.0 PgC yr^{-1} are applied if $T_{obs}(t)$ is less than ΔT_{aim} by more than 0.2 °C.

Alternative climate stabilization targets are achieved by altering the value of ΔT_{aim} in the algorithm (eqns. 1-3). Here, the AMPs are named according to the value of the climate stabilization target, ΔT_{aim}. AMP1.5 has climate stabilization ΔT_{aim} = 1.5 °C above preindustrial, AMP2.0 has climate stabilization ΔT_{aim} =2.0 °C above preindustrial, while AMP2.5, AMP3.0 and AMP4.5 have climate stabilization ΔT_{aim} at 2.5, 3.0 and 4.5 °C above preindustrial respectively (Figure 1).

3. Adjusting Mitigation Pathway scenarios to year 2300

This section presents the AMP scenarios for surface warming, carbon emissions, atmospheric CO_2, surface ocean acidification and sea-level rise for climate stabilization targets of 1.5 °C, 2.0 °C, 2.5 °C, 3.0 °C and 4.5 °C, and compares these to the projections for the high-end RCP8.5 scenario.

3.1 AMP scenario warming trajectories to year 2300

For AMP1.5, AMP2.0 and AMP2.5 the ensemble-median warming reaches the respective targets during the simulations (Figure 2), while for AMP3.0 the ensemble-median warming reaches 0.1 °C under target. For AMP4.5 the warming is still increasing as the simulations end, reaching 3.9 °C in 2300.

The AMP1.5 scenario overshoots 1.5 °C warming during the mid-21st century, with ensemble-median warming reaching 1.7 °C from the 2040s to the 2060s (Figure 2, gray), before relaxing back towards 1.5 °C warming by the 2140s.

AMP2.0 does not result in overshoot by the ensemble-median, with warming reaching 2.0 °C during the 2070s and remaining until the 2160s (Figure 2, blue). Eventually, warming relaxes down towards 1.8 °C by year 2300.

For the AMP2.5 scenario, the ensemble median warming remains under the 2.5 °C target through the 21st century, with warming reaching 2.3 °C by 2100 (Figure 2, orange). Ensemble-median warming eventually reaches the 2.5 °C target during the 2140s, before relaxing down to 2.3 °C warming by year 2300.

AMP3.0 sees ensemble-mean warming reach 2.4 °C by 2100. Ensemble-median warming then peaks at 2.9 °C from the 2190s to the 2210s (Figure 2, green), before stabilizing at 2.8 °C through to year 2300.

AMP4.5 sees warming increase over time throughout the simulations to year 2300, with ensemble-median warming reaching 2.5 °C at year 2100 and increasing to 3.9 °C at 2300 (Figure 2, red).

There is variation in the warming trajectories within the observation-consistent ensembles for each AMP warming target (Figure 2). For the pathways towards climate stabilization at 1.5, 2.0 or 2.5 °C, 66 % of the simulations cover a typical warming range of 0.6 °C while 95% of the simulations typically cover a warming range of 1.3 °C at year 2100. This reduces to 0.3 °C for 66% of simulations and 1.0 °C for 95 % of simulations at year 2300 (Figure 2). Thus, for climate stabilization targets of 2.5 °C or below, the AMP approach for carbon emissions reductions successfully deliver warming close to the policy target in the majority of the 5784 observation-consistent simulations.

3.2 AMP scenario emissions trajectories to year 2300

All the AMP scenarios follow a linear increase in emission rate towards the final INDC emissions (Fawcet et al., 2015) in year 2030 (Figure 3). After year 2030 the Adjusting Mitigation Pathway algorithm determines unique emissions trajectories for each of the 5,784 observation-consistent simulations within the ensemble depending on the warming target.

For climate stabilization at 1.5 °C, following AMP1.5, the ensemble-median emission rate is reduced to zero by year 2045 (Figure 3), with negative emissions of -1.0 PgC yr^{-1} required from 2046 to the 2120s as warming remains above the 1.5 °C target by more than 0.05 °C (Figure 2). Within the 5,784 ensemble simulations, the 1.5 °C target requires that the emission rate is reduced to zero in 66% of simulations between years 2041 and 2049.

For climate stabilization at 2.0 °C, the AMP2.0 scenario reduces the ensemble-median emission rate to half present-day levels during the 2060s and to zero during the 2080s (Figure 3). However, depending on the future temperature trajectory there is a wide range in when emissions must be reduced to zero: 5% of simulations see the emission rate reduced to zero by 2055, and 10% of simulations by 2057. This shows that the Paris Agreement commitment to restrict warming to 2.0 °C or less implies, depending on the realized warming between the 2003-2012 period and 2030, that the global net carbon emission rate may have to be reduced to zero during the 2050s.

The ensemble-median carbon emission rate is reduced to half the present value during the 2080s for stabilization towards 2.5 °C warming, AMP2.5 (Figure 3), during the 2140s for stabilization towards 3.0 °C warming, AMP3.0, and by 2200 for stabilization towards 4.5 °C warming, AMP4.5 (Figure 3). The ensemble-median emission rate reaches zero in the 2160s

for 2.5 °C stabilization and in the 2230s for 3.0 °C. Aiming for 4.5 °C warming allows the annual carbon emission rate to be reduced more slowly, with ensemble-median emissions remaining at 2 PgC yr^{-1} at in year 2300 (Figure 3).

3.3 Potential contribution from negative emissions

The AMP1.5 and AMP2.0 scenarios show that the ensemble-median global net carbon emission rate has to be reduced to zero (carbon neutrality) by year 2045 for AMP1.5 and by 2080 for AMP2.0, respectively (Figure 3). In addition, the AMP1.5 scenario requires negative emissions of -1.0 PgC yr^{-1} from 2046 to the 2120s (Figure 3). These two scenarios demand significant and sustained global mitigation of CO_2 emissions with reliance on long-term negative emissions for the AMP1.5 scenario. In terms of global mitigation, a phase-out of fossil fuels by 2045 (AMP1.5) or 2080 (AMP2.0) requires a rapid decarbonization of the power, industry, buildings and transport sectors. This may be accomplished by deep emission reductions through increasing shares of renewables, nuclear and carbon capture and storage of fossil fuel emissions in addition to increased energy efficiency. For net CO_2 emissions to become negative from 2046 onwards specific carbon dioxide removal technologies (CRD) have to be deployed (IPCC, 2014; Mathews, 2008; National Academy of Sciences, 2015; Tavoni & Socolow, 2013). Bioenergy with carbon capture and storage (BECCS) is the most widely selected negative emission technology (e.g. Azar et al., 2010; IPCC, 2014; Rao et al., 2008). Considering the AMP1.5 pathway, the question is how much BECCS can achieve in terms of negative emissions. The near-term mitigation rate of BECCS may be between 0.8 and 2.7 PgC yr^{-1} (IPCC, 2014) with a theoretical potential of up to 4.8 PgC yr^{-1} (Azar et al, 2010, Kriegler et al., 2013). This has to be put in perspective with the current net global carbon emission rate of 11.2 PgC yr^{-1} (Fig. 3). The large-scale deployment of BECCS has significant environmental impacts in terms of land use, water resources, and nutrients. For example, using switchgrass as a bioenergy feedstock would require $2x10^8$ ha of land, $4x10^3$ km^3 yr^{-1} of water and 20 Tg yr^{-1} of nitrogen fertilizer for removing 1 PtC yr-1 (Smith & Torn, 2013*)*. Thus the land area required for 1 PtC yr^{-1} removal is approximately 60% of the surface area of India. The AP1.5 scenario requires a steep cut in the global net carbon emission rate to reach carbon neutrality by 2045 (Figure 3). The theoretical potential for negative carbon emissions of BECCS with rates of up to 2.7 PgC yr^{-1} in the near term (IPCC, 2014) could result in significant cuts but it will most likely be constrained by the availability of land for energy crops, water resources and the use of fertilizer that results in additional non-CO_2 greenhouse gas emissions (Smith et al., 2015). Furthermore, BECCS directly competes with carbon capture and storage of fossil fuel emissions until they are phased-out. BECCS may provide the 1 PgC yr^{-1} negative emissions from 2045 onwards required by the AP1.5 pathway but given the significant impact of it on land, water and nutrients, it cannot significantly contribute to the reduction of global carbon emission from continuing use of fossil fuels between 2030 and 2045.

3.4 Robustness of AMP scenarios

The robustness of an adaptive policy pathway expresses the likelihood that the pathway will achieve its objectives, given the uncertainty in the system (e.g. Hasnoot et al., 2013). In this section we present evaluate how robust how the AMP scenarios are, both in terms of reaching the required warming target and in terms of assumptions made in generating the model ensembles.

3.4.1 Robustness to variation within the model ensemble

The ensemble of WASP simulations contains variation that spans observational uncertainty in observed historic warming, ocean heat uptake and atmosphere-ocean-terrestrial carbon fluxes (Supplementary Table 2), and incorporates the subset of geological uncertainty in climate sensitivity that is consistent with the historic period (Supplementary Table 1). The imposed stochastic temperature variability within each simulation (GISTEMP, 2017; Goodwin et al., 2018) also provides variation between simulations in how much the variability in surface

temperature affects the observed 10-year average surface warming at the t_n time periods (Figure 1).

Each simulation in the ensemble reacts differently to the AMP scenarios, representing uncertainty in the future of response of the physical climate system. We test the robustness of the AMP scenarios to this uncertainty (as encapsulated in the model ensemble) by assessing how many of the ensemble simulations reach the required warming target.

Table 1 shows the percentage of the 5784 ensemble simulations that are (i) within ±0.25 °C of the warming target or (ii) under the warming target for the AMP scenarios (AMP1.5, AMP2.0, AMP2.5, AMP3.0 and AMP4.5) for the twenty year periods at the end of the 21st, 22nd and 23rd centuries. For the AMP1.5 and AMP2.0 scenarios, over 64% of simulations are within ±0.25 °C of the warming target across all three time-averages. For scenarios with warming targets at 2.5 °C or greater (AMP2.5, AMP3.0 and AMP4.5), at least 75% of simulations are either less than, or within ±0.25 °C, of the warming target across all three time periods.

Despite the significant variation in the model ensemble (Tables A1, A2), the self-adjusting mechanisms within the AMP scenarios (equations 1-3) provide a robust method to achieve a policy driven warming target (Table 1).

3.4.2 Robustness of AMP method to alternative reduction pathways

In the standard AMP scenarios, equations (1) and (2) are used to evaluate from observations, at ten-year intervals (Fig. 1), how much future carbon can be emitted in total to stabilize climate at a given target. Equation (3) then calculates a linear reduction in the carbon emission (Fig. 2) to achieve this future total carbon emission (Fig. 3). However, a linear reduction in the carbon emission rate to zero is not the only policy option to achieve the determined total future carbon emission. An alternative policy option is to continually reduce the carbon emission rate by a calculated percentage year-on-year, such that the emission rate decays to zero with an e-folding timescale, $\tau_{remaining}$. To test the robustness of the Adjusting Mitigation Pathway approach to alternative policy choices for the way in which emissions are reduced, we conduct additional experiments in which emissions are reduced year-on-year, based on the observed warming, rather than linearly.

To generate these AMP scenarios with year-on-year reductions in the carbon emission rate, the following changes are made to the linear reductions approach. At each time, t_n, an e-folding timescale is adjusted such that the total future carbon emission is as determined by equations (1) and (2), using $\tau_{remaining} = I_{remaining}/C_{rate}(t_n)$, such that the total cumulative carbon emitted after t_n is equal to $I_{remaining}$. The annual carbon emission rate at time t, C_{rate}, is then reduced according to,

$$C_{rate}(t) = C_{rate}(t_n)\exp\left(\frac{-(t-t_n)}{\tau_{remaining}}\right), \qquad (4)$$

where and where the value of $I_{remaining}$ is evaluated in eqn. (2). Eqns. (1) (2) and (4) are applied to generate the Adjusting Mitigation Pathways using year-on-year reductions, again with ΔT_{aim} used to set the climate stabilization target. For these AMP scenarios with year-on-year emissions reductions AMP1.5yy has climate stabilization at 1.5 °C above preindustrial, and AMP2.0yy, AMP2.5yy, AMP3.0yy and AMP4.5yy have stabilization at 2.0, 2.5, 3.0 and 4.5 °C above preindustrial respectively (Figure 4a).

The AMP scenarios with year-on-year emission rate reductions have a quicker initial reduction in the emission rate than the linear reductions pathways, for the same warming

target (Figure 4a, compare solid lines to dashed lines). The year-on-year pathways then allow some continuation of emissions after the emission rate is brought to zero in the linear reductions pathways (Figure 4a, compare solid lines to dashed lines). This results in the warming targets being reached slightly later in the year-on-year reductions pathways, compared to the linear reductions pathways (Figure 4b, compare solid lines to dashed lines). However, across the same ensemble of model simulations the AMP scenarios with year-on-year emission-rate reductions have a similar success in getting to the required warming target as the AMP scenarios with linear emission-rate reductions (Table 1, e.g. compare AMP1.5yy to AMP1.5). Therefore, the AMP scenario methodology is robust to the choice of whether the emission rate is reduced linearly or with year-on-year emissions reductions. This is consistent with previous work indicating that it is the total amount of carbon emitted that is the primary control on the carbon-induced global mean surface warming (Allen et al, 2009; Gillet et al., 2013; Matthews et al. 2009; Goodwin et al., 2015).

3.4.3 Impact on robustness of inter-annual temperature variability

The imposed stochastic temperature variability within each simulation is chosen to approximate the observed monthly temperature variability in the GISTEMP record from 1971 to 2016 (GISTEMP, 2017; Goodwin et al., 2018).

An ensemble of year-on-year AMP scenarios is generated, differing only in that the AR2 noise on surface temperature is removed. In these 'no noise' ensemble simulations, the ability of the AMP algorithm to reach the target warming is slightly higher, but very similar to, the standard year-on-year AMP ensembles for each scenario: the maximum increase in the percentage simulations within ±0.25 °C for any time period is +3.8 %, while the average increase in the % simulations within ±0.25 °C across all three time periods and all 5 warming targets is just +1.3 %. Thus, the imposed temperature variability has minimal impact on the ability of the AMP scenarios to stabilize climate at their respective target warming levels.

We conclude that, in the ensemble of simulations, the inter-annual temperature variability as simulated in the model ensemble is not a significant factor in determining the robustness of the AMP method to successfully stabilize climate to a policy driven warming target. It should be noted though, that while the simulated inter-annual temperature variability in the WASP model approximates the observed amplitude for the real climate system from 1971 to 2016 (Goodwin et al., 2018), it may be that differences between future inter-annual variability in the real climate system and the WASP simulations may affect the robustness of the AMP scenarios for the real climate system.

3.4.4 Robustness to non-CO_2 radiative forcing

The AMP scenarios (Figures 1-4) assume that non-CO_2 radiative forcing follows the heavily mitigated RCP2.6 scenarios. However, it is not certain that such heavy mitigation will be applied to non-CO_2 agents. If less mitigation is applied to non-CO_2 radiative forcing agents than RCP2.6 going forward, then more mitigation must be applied to CO_2 emissions than the AMP scenarios suggest (Figures 3, 4a) to successfully reach the Paris Agreement warming targets (Figures 2, 4b).

To test how sensitive the required rates of carbon emission reductions are to the non-CO2 radiative forcing, we repeated the AMP scenario experiments with linear emission-rate reductions but, instead of applying RCP2.6 forcing for non-CO_2 agents, we applied the less-mitigated RCP4.5 forcing (Meinshausen et al., 2011a). This reduced the time required to reduce the emission rate to zero in the AMP scenarios by just 1 year when targeting 1.5 °C warming (from year 2045 for the ensemble-median in AMP1.5 to year 2044 with RCP4.5 forcing for non-CO_2 agents). However, to target 2 °C warming the reduction in mitigation in non-CO_2 agents required significantly more mitigation in the carbon emission rate: the time at which carbon emissions reached zero is brought forward by 27 years, from year 2087 for the ensemble-median in AMP2.0 to year 2060 with RCP4.5 forcing for non-CO_2 agents.

This substantial reduction in the time to reduce the emission rate to zero for a 2.0 °C warming target highlights the significant contribution to warming pathways that non-CO_2 forcing agents can make.

3.5 AMP scenarios for atmospheric CO_2 and surface ocean *p*H to year 2300

The preindustrial atmospheric CO_2 and global surface ocean *p*H values in the WASP model are 278 ppm and 8.2 respectively, with simulated values in year 2017 of 405 ppm for CO_2 and 8.06 for surface ocean *p*H. Now consider how the climate stabilization targets affect the future evolution of these quantities in the AMP scenarios.

Following AMP1.5 requires restricting ensemble-median atmospheric CO_2 to a peak of 450 ppm in year 2040 (Figure 5a), before reducing to around 410 ppm by year 2100 and 385 ppm by 2300. This sees the WASP ensemble-median surface-ocean *p*H reduce to a minimum 8.03 in year 2040 (Figure 5b), before increasing slightly to 8.05 in 2100 and 8.08 in year 2300. Targeting 2.0 °C warming requires restricting ensemble-median CO_2 to a peak of 475 ppm during the 2060s (Figure 5a) before eventually stabilizing at around 430 ppm by year 2300. Surface ocean *p*H reduces to a minimum of 8.00 in the 2060s before increasing towards 8.03 by year 2300.

Both AMP1.5 and AMP2.0 are in stark contrast to the unmitigated RCP8.5 scenario, which sees CO_2 increase to 935 ppm by year 2100 and 1960 ppm by year 2300 (Meinshausen et al., 2011a) (Figure 5a), with surface ocean pH decreasing to just 7.75 in year 2100 and 7.45 in year 2300 (Figure 5b). The much smaller decline in surface ocean pH for the AP scenarios compared to RCP8.5 (Figure 5b) shows the significant benefits of warming mitigation for also reducing ocean acidification. The additional benefit of restricting warming to 1.5 °C rather than 2.0 °C equates to around 0.05 *p*H units less surface acidification at stabilization (Figure 5b, compare gray to blue).

3.6 AMP scenarios for global mean sea-level rise to year 2300

Global mean sea level is calculated in the WASP Earth system model using a hybrid approach (Goodwin et al., 2017). A process-based thermosteric contribution, calculated from ocean heat uptake after Williams et al. (2012), is combined with a semi-empirical ice-melt contribution, calculated using the methodology of Rahmstorf (2007) but applied here only to ice-melt.

The sea-level projections made by the WASP model using this hybrid approach depend on the historical constraints used to extract the final WASP ensemble (Goodwin et al, 2017). If the historic constraints for sea-level rise are taken from from the process-based historic simulations of Assessment Report 5 (IPCC, 2013), then the21st century WASP sea-level projections also closely agree with Assessment Report 5 (Goodwin et al, 2017 – the 'SimHist' ensemble therein). However, if the historic constraints are taken from the observations of historic sea level rise, then the 21st century projections of the WASP ensemble are higher than the Assessment Report 5 projections (Goodwin et al, 2017 – see 'ObsHist' ensemble therein). Here, the historic sea-level rise constraints for the WASP model are taken from observations (Supplementary Table 2), and so the future sea level projections are slightly higher than other WASP ensembles where the historic constraints derive from the Assessment Report 5 process-base simulations (Goodwin et al, 2017, 'SimHist' ensemble, and Nicholls et al, 2018). It should be noted that there is discrepancy in the literature, with some studies projecting probability distributions containing considerably larger future sea-level projections than either Assessment Report 5 or the observationally constrained WASP projections used here (e.g. Kopp et al. 2017).

Up to year 2100 a constant value of the ice-melt coefficient may be assumed (Goodwin et al., 2017), defining the ice-melt contribution to the rate of sea-level rise per unit warming, in units of mm yr^{-1} $°C^{-1}$ (Goodwin et al., 2017; Rahmstorf, 2007). Here, to extend the sea level projections to year 2300, the ice-melt coefficient is reduced to zero over time after year 2100 following an exponential decay, such that the total ice-melt contribution to sea-level rise on a multi-millennial timescale is 2.3 m per °C global temperature anomaly (IPCC, 2013). The exponential decay timescale is set separately for each simulation. Based on a simulation's 21st century ice-melt coefficient value (Supplementary Table 1), the exponential decay timescale is set to the unique value that both avoids discontinuity in the ice-melt coefficient at year 2100 and reaches 2.3 m sea-level rise per °C temperature anomaly at equilibrium.

For the final WASP ensemble used here, the high-end RCP8.5 scenario sees ensemble-median GMSL rise of 0.78 m relative to the 1986-2005 average by year 2100 (Figure 6), with a 66% range from 0.62 m to 0.96 m and a 95% range from 0.50 m to 1.2 m. Median GMSL rise increases over time to around 2.5m by year 2200 and to around 4.5m by year 2300 (Figure 6).

Aiming for climate stabilization using the AMP scenarios for targets between 1.5 °C and 4.5 °C sees a significant reduction in GMSL rise relative to high-end RCP8.5 (Figure 6). Following the AMP to 1.5 °C avoids almost half of the high-end GMSL rise to 2100 (Figure 5), with ensemble-median GMSL rise reaching just 0.40m when aiming for 1.5 °C stabilization (66% range from 0.31m to 0.51m and 95% range from 0.24m to 0.66m). Aiming for 2.0 °C climate stabilization avoids nearly as much GMSL rise compared to business as usual, with ensemble–median GMSL rise of 0.46m at 2100 for AMP2.0 (66% range of 0.35 m to 0.57 m and 95% range from 0.27 m to 0.73 m).

The benefits of a lower climate stabilization target for reduced sea level rise continue to grow after year 2100 (Figure 6). For climate stabilization between 1.5 and 3.0 °C, every 0.5 °C reduction in the warming target reduces ensemble-median GMSL rise by 0.01 to 0.05 m by year 2100. This reduction in GMSL rise increases to 0.09 to 0.16 m by year 2200, and increases further to 0.18 to 0.26 m by year 2300 (Figure 6). For the year 2300, climate stabilization at 1.5 °C results in an average of 4 m reduction in GMSL compared to RCP8.5. Thus, the policy choices made this century to stabilize climate at reduced levels of surface warming will lead to growing benefits in terms of reduced GMSL rise for centuries to come.

4. Discussion and Conclusions

The Paris Agreement has focussed climate policy in terms of restricting the global surface temperature anomaly to a maximum of 2 °C above preindustrial, and preferably under 1.5 °C. While warming appears to be linearly related to cumulative carbon emissions, there is currently significant uncertainty in the sensitivity of this linear relationship (e.g. Allen et al, 2009; Gillet et al., 2013; Goodwin et al., 2015; IPCC, 2013; Matthews et al., 2009). The uncertainty makes it impossible to prescribe a carbon pathway policy now that both avoids the possible costs associated with warming exceeding the agreed target, and avoids the possible costs associated with cutting carbon emissions more than necessary.

This study has presented Adjusting Mitigation Pathway (AMP) scenarios, in which the carbon emission pathway is re-assessed every decade, starting at year 2030 after the Paris Agreement INDC period (UNFCCC, 2015), to steer the global surface temperature anomaly to the agreed policy target. The AMP scenarios are shown to work in a large ensemble of efficient Earth system model simulations, with simulations reaching the 1.5, 2.0 or 2.5 °C targets (Figure 2) due to the adjusting mitigation strategy (Figure 3).

If emissions follow the expected INDC path (Fawcet et al., 2015) to year 2030, our projections suggest it will take an enormous effort to keep warming from stabilizing above

1.5 °C (Figure 3, gray), with the required global net annual carbon emission rate reaching zero during the 2040s in most simulations. The pathway to climate stabilization at 2.0 °C warming is more achievable, with the global net carbon emission rate reaching zero in most simulations at some point between 2057 and the early 22nd century (Figure 3, blue). However, this does assume that non-CO_2 radiative forcing agents are also heavily mitigated. If there is less mitigation on non-CO_2 agents then carbon emissions will have be reduced to zero more quickly, potentially by decades.

Both the AMP scenarios for the 1.5 °C and 2.0 °C warming targets have considerable benefits in terms of surface ocean *p*H and sea-level rise compared to a higher warming target or a high-end prescribed scenario, RCP8.5 (Figs. 5 and 6). While the benefits in terms of reduced ocean acidification are felt immediately as the emissions pathways diverge (compare Figures 3 and 5), the benefits of reduced sea-level rise continue to grow over the coming centuries even after emissions cease (compare Figures 3 and 6).

Our self-adjusting approach to mitigation provides policy makers and stakeholders with a framework to achieve their agreed warming targets, based on a decadal timescale for pathway re-assessment. The AMP scenarios we have presented show the impact of the agreed climate stabilization target for carbon emissions, surface warming, atmospheric CO_2, surface ocean *p*H and global mean sea-level rise (Electronic Supplementary Information). We anticipate that this information will allow a wide variety of stakeholders to assess how the climate stabilization target has knock-on effects for these other parameters.

Acknowledgements and Data:

This research was funded by the joint United Kingdom Natural Environment Research Council and United Kingdom Government Department of Business Energy & Industrial Strategy grant "ADJUST1.5", numbered NE/P01495X/1. PG acknowledges support from UK Natural Environment Research Council grant number NE/N009789/1. The authors declare no competing financial interests.

The datasets describing the Adjusting Mitigation Pathway (AMP) scenarios developed here are available in Electronic Supplementary Information. File Goodwinetal-ds01.xlsx contains the AMP carbon emissions scenarios, file Goodwinetal-ds02.xlsx contains the AMP surface warming scenarios, file Goodwinetal-ds03.xlsx contains the AMP atmospheric CO_2 scenarios, file Goodwinetal-ds04.xlsx contains the AMP surface ocean *p*H scenarios, and file Goodwinetal-ds05.xlsx contains the AMP Global Mean Sea Level scenarios. Each file contains values from the WASP ensemble used in the study to generate Figures 1-5 and gives a range of percentiles from the WASP simulations to provide uncertainty estimates. File Goodwinetal-ds06.xlsx and Goodwin et al-ds07.xlsx contain the carbon emission scenarios and surface warming scenarios respectively for the AMP scenarios with year-on-year emissions reductions.

References:

Allen, M. R., Frame1, D.J., Huntingford, C., Jones, C.D., Lowe, J.A., Meinshausen, M. & Meinshausen, N. (2009), Warming caused by cumulative carbon emissions towards the trillionth tonne. *Nature* 458, 1163-1166, doi:10.1038/nature08019.

Azar, C. Lindgren, K., Michael Obersteiner, M., Riahi, K., van Vuuren, D.P., den Elzen, K.M.G.J. … Larson, E.D. (2010) The feasibility of low CO*2* concentration targets and the role of bio-energy carbon capture and storage. *Clim. Change* 100, 195-202.

Barnett, J., Graham, S., Mortreux, R., Fincher, R., Waters, E. and Hurlimann, A. (2013). A local coastal adaptation pathway. *Nature Climate Change*, doi: 10.1038/nclimate2383

Boden, T.A., Marland, G. & Andres, R.J. (2016), *Global, Regional, and National Fossil-Fuel CO2 Emissions*. Carbon Dioxide Information Analysis Center, Oak Ridge National Laboratory, U.S. Department of Energy, Oak Ridge, Tenn., U.S.A. doi:10.3334/CDIAC/00001_V2016

Cheng, L., Trenberth, K.E., Fasullo, J., Boyer, T., Abraham, J. & Zhu, J. (2017), Improved estimates of ocean heat content from 1960 to 2015. *Science Advances,* 3.3, e1601545, doi: 10.1126/sciadv.1601545 .

Church J.A. & White, N. J. (2011), Sea-Level Rise from the Late 19th to the Early 21st Century, *Surveys in Geophysics*, 32, 585-602, doi: 10.1007/s10712-011-9119-1.

Fawcet, A.A. *et al* (2015) Can Paris pledges avert severe climate change? *Science* 350*,* 1168–1169, doi:10.1126/science.aad5761

Gillet, N. P., Arora, V. K., Matthews, D. & Allen, M. R. (2013), Constraining the ratio of global warming to cumulative CO2 emissions using CMIP5 simulations. *J. Climate* 26, 6844-6858.

GISTEMP Team: *GISS Surface Temperature Analysis (GISTEMP)* (2017), NASA Goddard Institute for Space Studies. Dataset accessed 2017-01-19 at https://data.giss.nasa.gov/gistemp/.

Goodwin, P. (2016), How historic simulation-observation discrepancy affects future warming projections in a very large model ensemble, *Clim. Dyn*., 47(7), 2219–2233, doi:10.1007/s00382-015-2960-z.

Goodwin, P., Williams, R.G. , and Ridgwell, A. (2015), Sensitivity of climate to cumulative carbon emissions due to compensation of ocean heat and carbon uptake, *Nature Geoscience* 8, p29-34. doi:10.1038/ngeo2304.

Goodwin, P., Haigh, I. D. , Rohling, E. J. , & Slangen, A. (2017), A new approach to projecting 21st century sea-level changes and extremes, *Earth's Future*, 5,240–253, doi:10.1002/2016EF000508.

Goodwin, P., Katavouta, A., Roussenov, V.M., Foster, G.L., Rohling, E.J., and Williams, R.G. (2018), Pathways to 1.5 and 2 °C warming based on observational and geological constraints, *Nature Geoscience*, doi:10.1038/s41561-017-0054-8.

Haasnoot, M. Kwakkel, J.H., Walker, W.E., ter Maat, J. (2013). Dynamic adaptive policy pathways: A method for crafting robust decisions for a deeply uncertain world, *Global Environmental Change*, 23, 2, 485-498, doi: 10.1016/j.gloenvcha.2012.12.006.

Hansen J., Ruedy, S., Sato, M. & Lo, K. (2010), Global surface temperature change*, Rev. Geophys.*, 48, RG4004.

Houghton, R.A., van der Werf, G.R., DeFries, R.S., Hansen, M.C., House, J.I., Le Quéré, C., Pongratz, J. & Ramankutty, N. (2012). Chapter G2 Carbon emissions from land use and land-cover change, *Biogeosciences*, 9, 5125-514.

IPCC (2013), *Climate Change 2013: The Physical Science Basis. Contribution of Working Group I to the Fifth Assessment Report of the Intergovern- mental Panel on Climate Change* [Stocker, T.F., D. Qin, G.-K. Plattner, M. Tignor, S.K. Allen, J. Boschung, A. Nauels, Y. Xia,

V. Bex and P.M. Midgley (eds.)]. Cambridge University Press, Cambridge, United Kingdom and New York, NY, USA, 1535 pp.

IPCC (2014), *Climate Change 2014: Mitigation of Climate Change. Contribution of Working Group III to the Fifth Assessment Report of the Intergovernmental Panel on Climate Change* [Edenhofer, O., R. Pichs-Madruga, Y. Sokona, E. Farahani, S. Kadner, K. Seyboth, A. Adler, I. Baum, S. Brunner, P. Eickemeier, B. Kriemann, J. Savolainen, S. Schlömer, C. von Stechow, T. Zwickel and J.C. Minx (eds.)]. Cambridge University Press, Cambridge, United Kingdom and New York, NY, USA.

Kopp, R. E., DeConto, R. M., Bader, D. A., Hay, C. C., Horton, R. M., Kulp, S., Oppenheimer, M., Pollard, D., & Strauss, B. H. (2017). Evolving Understanding of Antarctic Ice-Sheet Physics and Ambiguity in Probabilistic Sea-Level Projections, *Earth's Future*, 5, 1217–1233, doi:10.1002/2017EF000663.

Kriegler, E., Tavoni, M., Aboumahboub, T., Luderer G., Calvin, K., Demaere, G., … van Vuuren, D.P. (2013), What does the 2ºC target imply for a global climate agreement in 2020? The LIMITS study on Durban Platform scenarios. *Clim. Change Econ.* 04 1340008. doi: 10.1142/S2010007813400083.

Le Quéré, C., Andrew, R.M., Canadell, J.G., Sitch, S., Korsbakken, J.I. Peters, G.P. … Zaehle, S. (2016). Global Carbon Budget 2016, *Earth Syst. Sci. Data*, 8, 605-649, doi:10.5194/essd-8-605-2016.

Levitus, S., Antonov, J. I., Boyer, T. P., Baranova, O.K., Garcia, H.E., Locarnini, R. A.,… Zweng, M. M. (2012), World ocean heat content and thermosteric sea level change (0–2000 m), 1955–2010, *Geophys. Res. Lett.* 39.10.

Matthews, H.D., Gillet, N. P., Stott, P. A. & Zickfield, K. (2009), The proportionality of global warming to cumulative carbon emissions. *Nature* 459, 829-832.

Mathews, J.A. (2008), Carbon-negative biofuels. *Energy Policy* 36(3), 940-945.

Meinshausen, M., Meinshausen, N., Hare, W., Raper, S.C.B., Frieler, K., Knutti, R., … Allen, M. R. (2009). Greenhouse-gas emission targets for limiting global warming to 2°C. *Nature*, 458, 1158–1162.

Meinshausen M, Smith, S. J., Calvin, K., Daniel, J. S., Kainuma, M.L.T. Lamarque, J-F., … van Vuuren, D.P.P., (2011a). The RCP greenhouse gas concentrations and their extensions from 1765 to 2300. *Clim. Change*, 109, 213–241, doi:10.1007/s10584-011-0156-z.

Meinshausen, M., Raper, S. C. B., and Wigley, T. M. L., (2011b). Emulating coupled atmosphere-ocean and carbon cycle models with a simpler model, MAGICC6 – Part 1: Model description and calibration, *Atmos. Chem. Phys.*, 11, 1417-1456, https://doi.org/10.5194/acp-11-1417-2011, 2011.

Meinshausen, M., Wigley, T. M. L., and Raper, S. C. B., (2011c). Emulating atmosphere-ocean and carbon cycle models with a simpler model, MAGICC6 – Part 2: Applications, Atmos. Chem. Phys., 11, 1457-1471, https://doi.org/10.5194/acp-11-1457-2011.

Morice, C. P., Kennedy, J. J. , Rayner, N. A. & Jones, P. D. (2012), Quantifying uncertainties in global and regional temperature change using an ensemble of observational estimates: the HadCRUT4 dataset, *J. Geophys. Res.*, 117, D08101, doi:10.1029/2011JD017187. Dataset accessed 2017-01-19 at https://crudata.uea.ac.uk/cru/data/temperature/

National Academy of Sciences (2015), Climate Intervention: Carbon Dioxide Removal and Reliable Sequestration, *National Academies Press*.

Nicholls, R.J., Brown, S., Goodwin, P., Wahl, T., Lowe, J., Solan, M. … Merkens, J.-L. (2018, in review) Stabilisation of global temperatures at 1.5°C and 2.0°C: Implications for coastal areas, *Phil. Trans. R. Soc. A.*

Nicholls, R.J., Reeder, T., Brown, S. and Haigh, I.D. (2015). The risks of sea-level rise for coastal cities. In, King, David, Schrag, Daniel, Dadi, Zhou, Ye, Qi and Ghosh, Arunabha (eds.) Climate change: a risk assessment. London, GB, Foreign and Commonwealth Office, 94-98.

Rahmstorf, S. (2007), A semi-empirical approach to projecting future sea-level rise, *Science*, 315, 368–370, doi:10.1126/science.1135456.

Ranger, N., Reeder, N. and Lowe, J. (2013). Addressing 'deep' uncertainty over long-term climate in major infrastructure projects: four innovations of the Thames Estuary 2100 Project. *EURO J Decis Process*, 1, 233–262, doi:10.1007/s40070-013-0014-5.

Rao, S., Riahi, K., Stehfest, E., van Vuuren, D.P., Cho, C., Elzen, M.G.J. den, … van Vliet, J. (2008), IMAGE and MESSAGE scenarios limiting GHG concentration to low levels. *IIASA Interim Report IR-08-020*. International Institute for Applied Systems Analysis, Laxenburg, Austria.

Rohling, E. J., Sluijs, A., Dijkstra, H. A., Köhler, P., van de Wal, R. S. W., … Zeebe, R.E. (2012), Making sense of palaeoclimate sensitivity, *Nature* 491, 683-691, doi:10.1038/nature11574.

Smith, D. M. & Murphy, J. M. (2007), An objective ocean temperature and salinity analysis using covariances from a global climate model. *J. Geophys. Res.,* 112, C02022, doi:10.1029/2005JC003172.

Smith, L.J. and Torn, M.S. (2013), Ecological limits to terrestrial biological carbon dioxide removal. *Clim. Change* 118, 89-103.

Smith T. M., Reynolds, R. W., Peterson, T. C. & Lawrimore, J. (2008), Improvements to NOAA's historical merged land–ocean surface temperature analysis (1880–2006), *J. Clim.*, 21, 2283–2296.

Smith, D.M., Allan, R.P., Andrew C Coward,A.C., Eade, R., Hyder, P., Liu, C., … Scaife, A.A. (2015), Earth's energy imbalance since 1960 in observations and CMIP5 models. *Geophys. Res. Let.,* 42.4: 1205-1213.

Tavoni. M. & Socolow, R. (2013) Modeling meets science and technology: An introduction to a special issue on negative emissions. *Clim. Change* 118, 1-14.

UNFCCC (2015). Adoption of the Paris Agreement. Report No. FCCC/CP/2015/L.9/Rev.1, http://unfccc.int/resource/docs/2015/cop21/eng/l09r01.pdf

Vose R. S., Arndt, D., Banzon, V.F., Easterling, D.R., Gleason, B., Huang, B., … Wuertz, D.B.. (2012), NOAA's merged land-ocean surface temperature analysis. *Bulletin Amer. Meteorol. Soc.*, **93**, 1677–1685, doi:10.1175/BAMS-D-11-00241.1.

906 Williams, R. G., Goodwin, P., Ridgwell, A., and Woodworth, P. L. (2012), How warming and steric sea level rise relate to cumulative carbon emissions, *Geophys. Res. Lett.*, 39, L19715,
908 doi:10.1029/2012GL052771.

910 Williams, R. G., Goodwin, P., Roussenov, V.M. & Bopp, L. (2016), A framework to understand the Transient Climate Response to Emissions. *Environmental Research Letters*,
912 11, doi:10.1088/1748-9326/11/1/015003.

914 Williams, R.G., Roussenov, V., Goodwin, P. , Resplandy L. & Bopp, L. (2017), Sensitivity of global warming to carbon emissions: effects of heat and carbon uptake in a suite of Earth
916 system models. *J. Climate*, doi: 10.1175/JCLI-D-16-0468.1.

918 Williamson, D., Goldstein, M., Allison, L., Blaker, A., Challenor, P., Jackson, L., & Yamazaki, K. (2013), History matching for exploring and reducing climate model parameter
920 space using observations and a large perturbed physics ensemble, *Clim. Dyn.,* 41, 1703-1729, doi:10.1007/s00382-013-1896-4,
922
Williamson, D., Blaker, A.T., Hampton, C., & Salter, J. (2015), Identifying and removing
924 structural biases in climate models with history matching, *Clim. Dyn.,* 45, 1299, doi:10.1007/s00382-014-2378-z.
926

928
Figures, Tables and Captions
930

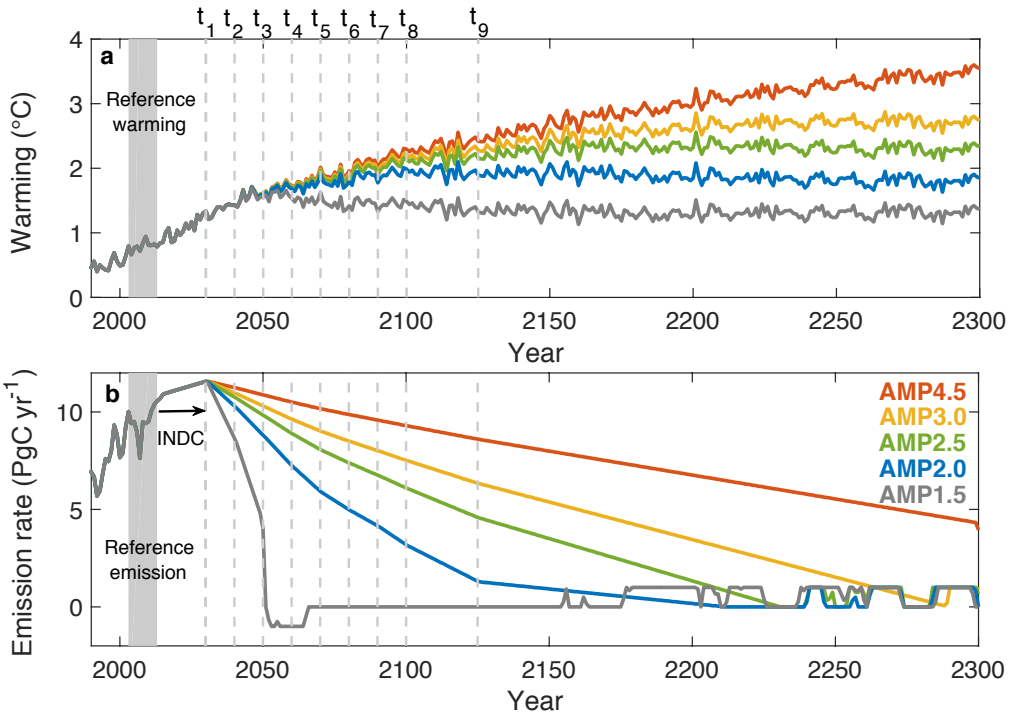

932 Figure 1: Adjusting Mitigation Pathways towards climate stabilization at different warming targets in a model simulation. (a) Warming and (b) CO_2 emission rate over time. Shown is a
934 single WASP Earth system model simulation following 5 AMP scenarios (solid lines) for warming targets of 1.5, 2.0, 2.5, 3.0 and 4.5 °C. The AMP algorithm determines the emissions
936 reduction pathway to reach the required warming target at 10-year intervals from year t_1=2030 to year t_8=2100, and again at year t_9=2125 (grey dashed lines) by considering the
938 additional warming and emissions since a reference period (gray solid bar).

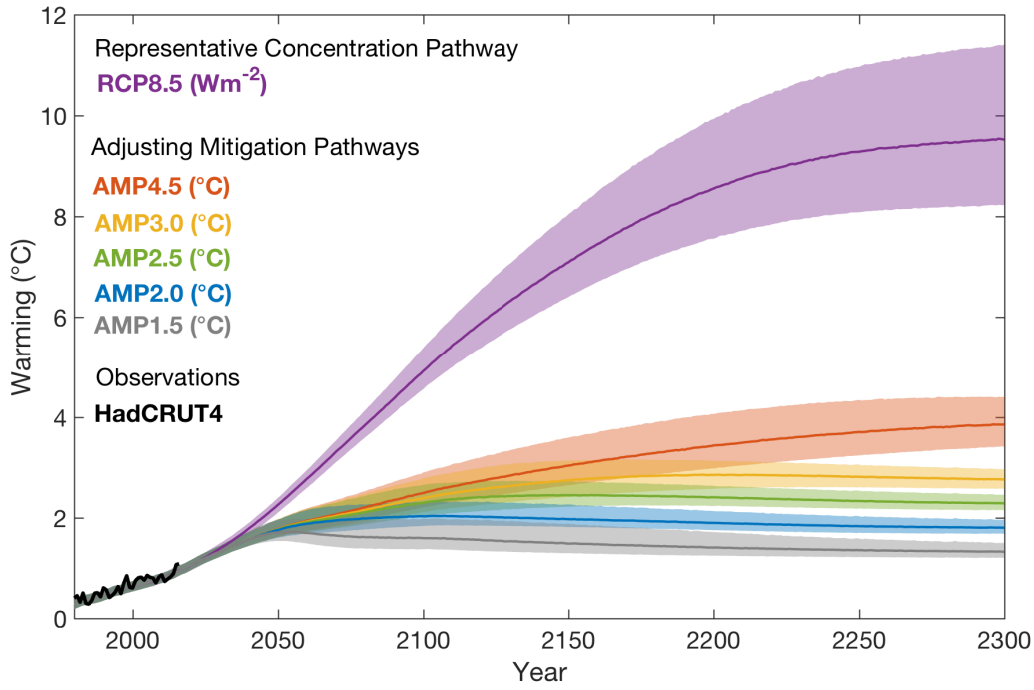

Figure 2: Global mean surface temperature anomaly relative to 1850-1900 average from observations and for Earth system model projections. For the simulations, the lines are the ensemble medians and the shaded regions are the 66% ranges (from the 17th to 83rd percentiles). The observations (black line) are from the HadCRUT4 dataset (*Morice et al.*, 2012).

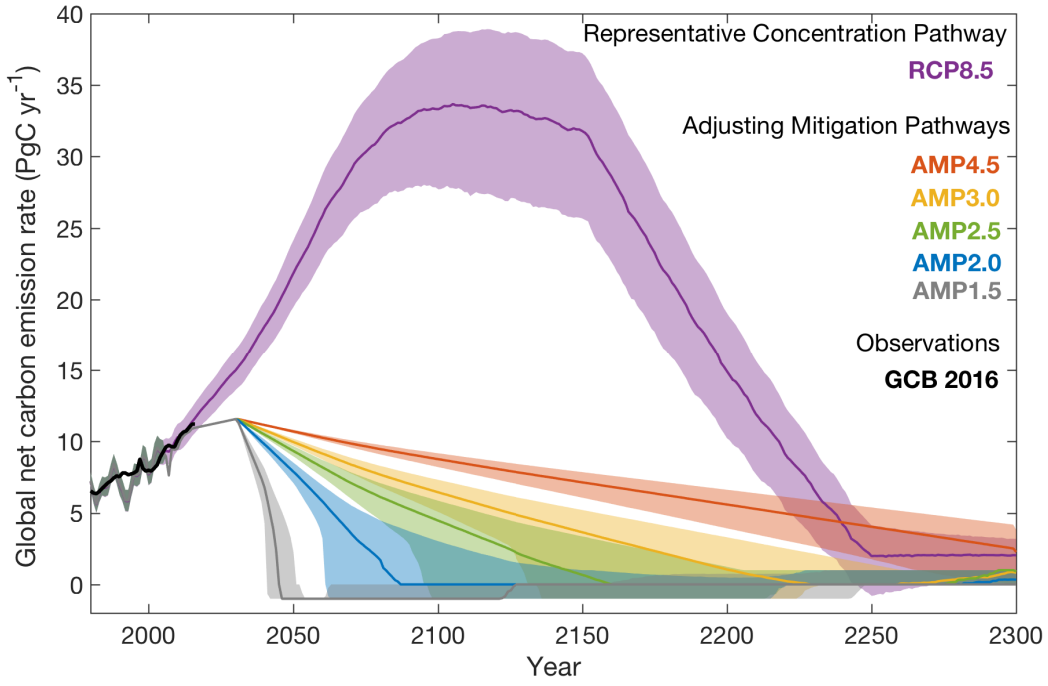

Figure 3: The global net carbon dioxide emission rate (PgC yr^{-1}) over time from observations and for alternative scenarios in the observation-constrained WASP ensemble. Observations stem from the Global Carbon Budget 2016 (le Quere et al., 2016). Shading and colors are as Figure 2.

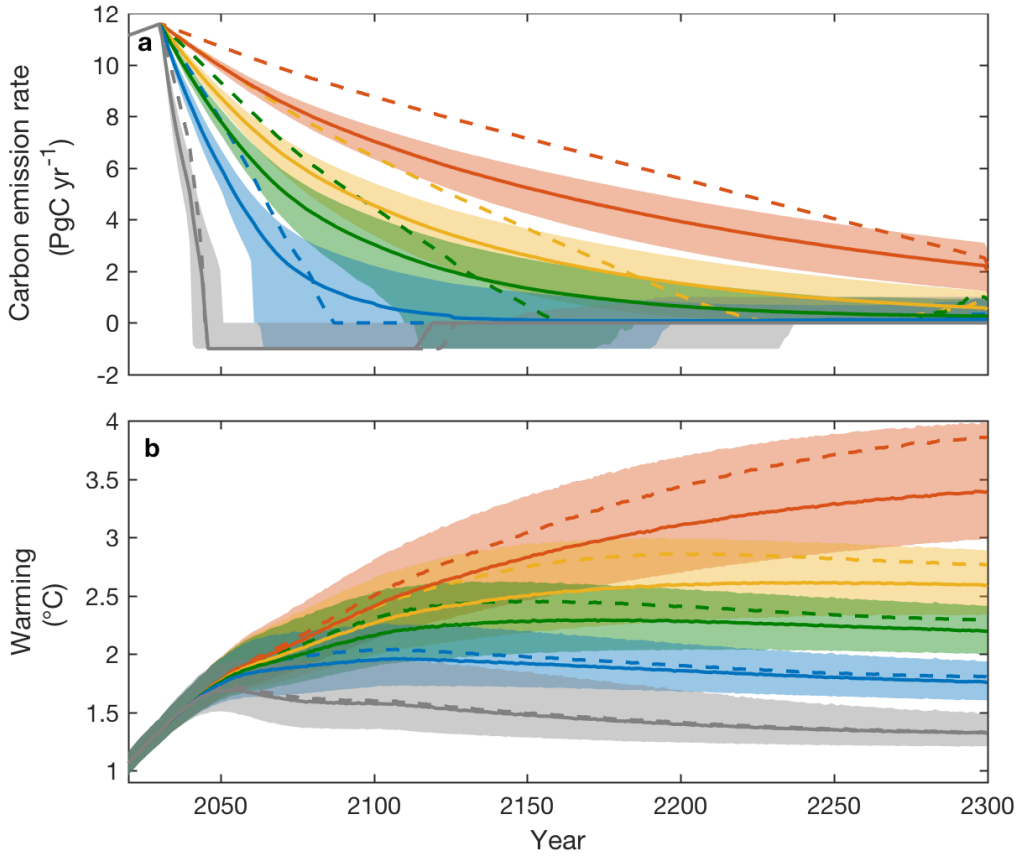

Figure 4: Ensemble projections of (a) carbon emission rate and (b) surface warming for AMP scenarios with year-on-year emissions reductions (solid lines, shading) compared to linear emissions reductions (dashed lines). Colors for warming targets and shading for ensemble ranges are as Figure 2, but here are shown for the AMP scenarios with year-on-year emissions reductions: AMP1.5yy (gray), AMP2.0yy (blue), AMP2.5yy (green), AMP3.0yy (yellow) and AMP4.5yy (red). Dashed lines show the ensemble median for the linear reductions scenarios, shown in Figures 2 and 3, for comparison.

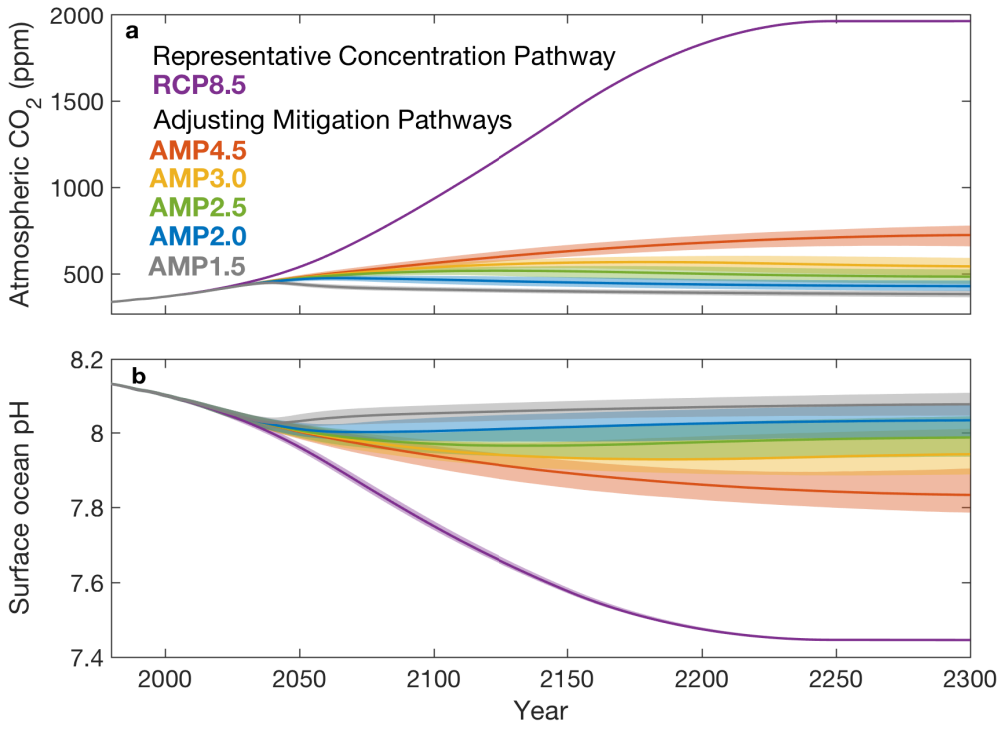

Figure 5: AMP scenarios for atmospheric CO_2 and surface ocean acidification. Colours and shading as Figure 2.

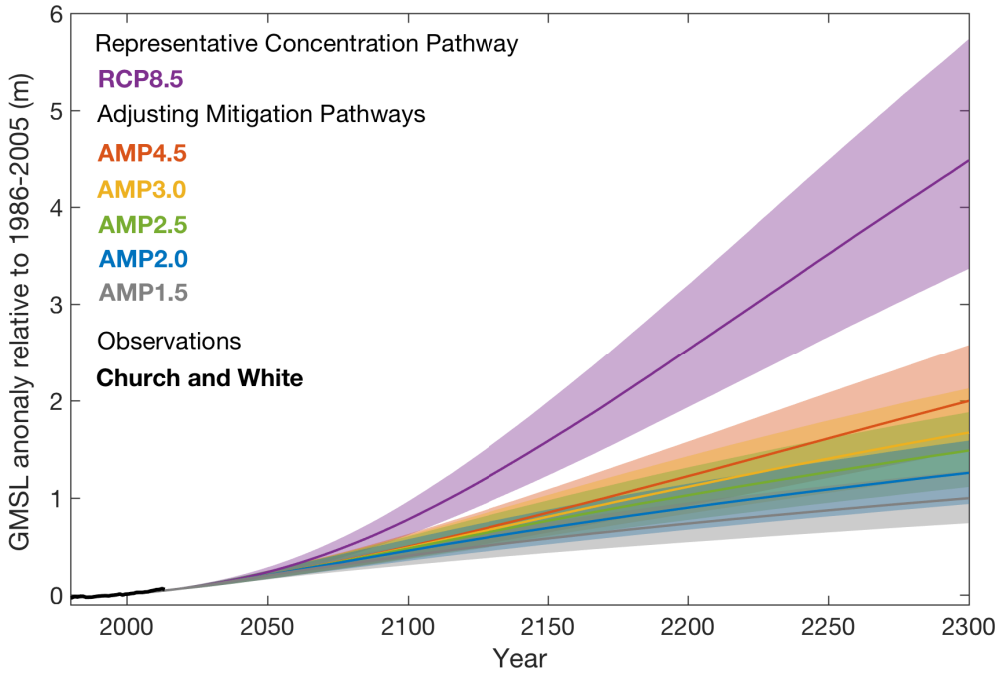

Figure 6: The Global Mean Sea Level anomaly relative to 1986-2005 (m) over time from observations and future scenarios in an Earth system model. The period from years 1980 to 2300 is shown. The observation GMSL reconstruction is from Church and White (2011), downloaded 10th May 2017. Shading and colors are as Figure 2.

	% of simulations with 20-year average temperature within ±0.25 °C of target (% of simulations below target)		
	2081-2100	**2181-2200**	**2281-2300**
AMP1.5	64.8 (33.3) %	71.6 (64.8) %	75.5 (85.7) %
AMP1.5yy	66.2 (37.6) %	71.8 (67.3) %	75.6 (87.2) %
AMP2.0	73.6 (46.6) %	79.3 (70.7) %	69.1 (89.5) %
AMP2.0yy	63.8 (60.1) %	66.4 (75.7) %	52.6 (91.4) %
AMP2.5	38.9 (79.5) %	75.1 (68) %	61.4 (89.6) %
AMP2.5yy	27.1 (86.7) %	48.8 (78.6) %	39.1 (92.3) %
AMP3.0	9.4 (95.8) %	53.6 (69.7) %	52 (87.5) %
AMP3.0yy	6.4 (97.4) %	28 (84.2) %	28.7 (91.7) %
AMP4.5	0 (100) %	6.7 (94) %	18.8 (87.4) %
AMP4.5yy	0 (100) %	3.3 (97.2) %	7.1 (94.8) %

Table 1. Robustness of the Adjusting Mitigation Pathways for reaching target warming in the climate model ensemble in three twenty-year average periods. The percentage of the ensemble simulations that have 20-year average temperature anomalies within ±0.25 °C of the target, and the % of ensemble simulations below the target, are shown for the AMP scenarios with linear emissions reductions and year-on-year emissions reductions.

Supplementary Tables:

Model parameter	Input distribution	Reference/comment
Radiative forcing coefficient from CO_2, a (Wm^{-2})	Normal distribution: μ=5.35 Wm^{-2}, σ=0.27 Wm^{-2}	From AR5 estimate of the parameter (IPCC, 2013)
Radiative forcing from CH_4, N_2O and halogens in 2011 (Wm^{-2}).	Normal distribution: μ= 1.01 Wm^{-2}, σ = 0.061 Wm^{-2}	To approximate AR5 estimate of radiative forcing from non-CO_2 Well Mixed Greenhouse Gases in 2011 (IPCC, 2013)
Radiative forcing from aerosols (and other agents outside the Kyoto Protocol), in 2011 (Wm^{-2}) $\Delta R_{aero}(t$=2011)	Randomly drawn from normal distribution: μ= -0.9 Wm^{-2}, σ = 0.61 Wm^{-2}	To approximate AR5 estimate of radiative forcing from aerosols in 2011 from IPCC (2013).
Climate Sensitivity, S (K $(Wm^{-2})^{-1}$)	Cenozoic distribution with log-normal uncertainty (Figure 3a, black)	Distribution from Rohling et al (2012) with log-normal uncertainty.
Ice-melt sea level rise coefficient, c_{ice}	Uniform distribution: 0.5 to 5.0 mm yr^{-1} K^{-1}	Distribution as WASP experiments in *Goodwin et al*. (2017)
Thermosteric sea level rise coefficient, c_{therm}	Normal distribution: μ= 1.4 mm yr^{-1} $(Wm^{-2})^{-1}$, σ= 0.3 mm yr^{-1} $(Wm^{-2})^{-1}$	Distribution as in WASP experiments in Goodwin et al (2017), from steric sea level rise arguments from Williams et al. (2012).
Relative efficacy of ocean heat uptake, ε_N	Uniform distribution: 0.33 to 3.0.	Allows ocean heat uptake to have between one-third to three times the impact on warming compared to an equal radiative forcing from CO_2.
Ratio of warming between global surface air temperatures and global sea surface temperatures at equilibrium, r_1	Uniform distribution: 0.30 to 1.45	Tuned to encompass all observationally consistent ensemble members (i.e. wider ranges receive no additional ensemble members that are observationally consistent)
Ratio of warming between global whole-ocean warming and global sea surface warming at equilibrium, r_2	Uniform distribution: 0.01 to 0.75.	Tuned to encompass all observationally consistent ensemble members (as above)
Fraction of total Earth system heat uptake that enters the ocean, f_{heat}	Uniform distribution: 0.9 to 0.96	Centred on the estimate of 93% of total Earth system heat uptake by the ocean from IPCC (2013)
The sensitivity of global Net Primary Production to temperature anomaly, ∂NPP/∂T (PgC yr^{-1} $°C^{-1}$)	Uniform distribution: –5.0 to 1.0 PgC yr^{-1} $°C^{-1}$	As per WASP experiments in *Goodwin* (2016)
The sensitivity of global soil carbon residence time to global temperature anomaly, $\partial\tau_{soil}/\partial$T (yr $°C^{-1}$)	Uniform distribution: -2.0 to 1.0 yr $°C^{-1}$	As per WASP experiments in *Goodwin* (2016)
The CO_2 fertilisation coefficient	Uniform distribution: 0 to 1.	As per WASP experiments in Goodwin (2016)
The buffered carbon inventory of the air-sea system, I_B	Uniform distribution: 3100 to 3900 PgC	As per WASP experiments in Goodwin (2016) and Goodwin et al. (2017)
e-folding timescale for tracers to equilibrate between the surface mixed layer and the atmosphere	Uniform distribution: 0.1 to 0.5 yr.	As per WASP experiments in Goodwin (2016) and Goodwin et al. (2017)
e-folding timescale for tracers to equilibrate between the surface mixed layer and the upper ocean	Uniform distribution: 5 to 40 yr.	As per WASP experiments in Goodwin (2016) and Goodwin et al. (2017)
e-folding timescale for tracers to equilibrate between the surface mixed layer and the intermediate ocean	Uniform distribution: 15 to 60 yr.	As per WASP experiments in Goodwin (2016) and Goodwin et al. (2017)
e-folding timescale for tracers to equilibrate between the surface mixed layer and the deep ocean	Uniform distribution: 75 to 500 yr.	As per WASP experiments in Goodwin (2016) and Goodwin et al. (2017)
e-folding timescale for tracers to equilibrate between the surface mixed layer and the bottom ocean	Uniform distribution: 250 to 1500 yr.	As per WASP experiments in Goodwin (2016) and Goodwin et al. (2017)

Supplementary Table 1: Model input distributions in the initial 50,000,000 WASP simulations.

988

990

992

Climate system observation	Observational consistency test	Reference/Comment
Surface temperature anomaly, 1850-1900 to 2003-2012	0.72 to 0.85 °C	IPCC (2013)
Surface temperature anomaly, 1951-1960 to 2007-2016	0.59 to 0.73 °C	Range encompasses HadCRUT4, NASA GISTEMP and NCDC reconstructions (Morice et al, 2012; GISTEMP, 2017; Hansen et al, 2010; Smith et al, 2008; Vose et al, 2012)
Surface temperature anomaly, 1971-1980 to 2007-2016	0.61 to 0.64 °C	Range encompasses HadCRUT4, NASA GISTEMP and NCDC reconstructions (GISTEMP, 2017; Hansen et al, 2010; Morice et al, 2012; Smith et al, 2008; Vose et al, 2012)
Sea Surface Temperature anomaly, 1850-1900 to 2003-2012	0.56 to 0.68 °C	Mean of HadSST3 and ERSST records, with ±0.06 °C uncertainty to reflect uncertainty in global temperature anomaly. (IPCC, 2013; Morice et al, 2012; Smith et al, 2008; Vose et al, 2012)
Heat content anomaly in upper 700m of the ocean, 1971 to 2010	98 to 170 ZJ	Range encompasses NODC, Cheng et al. and MOSORA reconstructions (Cheng et al, 2017; Levitus et al, 2012; Smith et al, 2015; Smith and Murphy, 2007)
Whole ocean heat content anomaly, 1971 to 2010	117 to 332 ZJ ($1\ ZJ=10^{21}J$)	Range encompasses NODC, Cheng et al. and MOSORA reconstructions (Cheng et al, 2017; Levitus et al, 2012; Smith et al, 2015; Smith and Murphy, 2007)
Cumulative ocean anthropogenic carbon sink, 1750 to 2011	125 to 185 PgC	IPCC (2013)
Cumulative residual-terrestrial anthropogenic carbon sink, 1750 to 2011	70 to 250 PgC	IPCC (2013)
Residual-terrestrial anthropogenic carbon sink, 2000 to 2009	1.4 to 3.8 PgC yr^{-1}	IPCC (2013)
Global Mean Sea Level rise from 1993 to 2012 (excluding contribution from changes in land-water storage).	1.9 to 3.2 mm yr^{1}	IPCC (2013)

Supplementary Table 2: The observational consistency tests used to select the observation-consistent WASP ensemble from the initial 50,000,000 simulations.

994